Photoinduced Crystallization of Amorphous Ice Films on Graphite

Dinko Chakarov* and Bengt Kasemo

Department of Applied Physics, Chalmers University of Technology and University of Göteborg, 412 96 Göteborg, Sweden

(Received 15 June 1998)

We have experimentally discovered a new nonthermal mechanism by which submonolayer and multilayer amorphous ice films, deposited at $T < 100$ K, crystallize due to UV radiation; the proposed mechanism is that photoexcited charge carriers in the graphite substrate tunnel into defect states in the amorphous film, and induce exothermic relaxation from the metastable amorphous to the stable crystalline phase. [S0031-9007(98)07899-5]

PACS numbers: 68.35.Rh, 73.50.Gr, 82.50.Fv

The structure and structural transformations of thin ice films at <150 K currently receive high interest [1,2]. A specific example [3–5] is the substrate-specific structure and structural transformations of thin ice films on different supports at 90–150 K: Ice grows amorphous in a metastable phase below 100–120 K and crystalline above 130–140 K. Heating of the amorphous ice films to >130 K induces a weakly exothermic transition from the amorphous to the crystalline phase (on graphite the activation energy for this transition is about 0.4 eV).

Besides the general interest in the physics and chemistry of water [6,7], these studies are also motivated by the special role of ice films in ozone depletion chemistry, cometary science, and astrophysics [8,9]. For example, the structure state of ice influences both its chemical properties [10] and vapor pressure [11,12]. The latter in turn affects the mass balance between gaseous and solid water. It is thus of central importance for both stratospheric chemistry and astrophysics [13] to understand at what conditions ice films appear in different structural states, and to unravel mechanisms that cause phase transformations between them.

We have discovered that low energy UV light transforms amorphous ice films to high coordinated, quasicrystalline ice. The model system is thin ice films [0.1–10 monolayers (ML)] deposited around 90 K on the graphite (0001) surface [highly oriented pyrolytic graphite (HOPG)]. The experiments were performed in an UHV chamber with base pressure $\leq 2 \times 10^{-10}$ torr. The photon source was a Hg arc lamp system and a combination of bandpass and cutoff filters with photon fluxes in the range $(1.6–2.4) \times 10^{16}$ photons cm^{-2} s^{-1} for 220–600 nm photons. The ice films were deposited from an effusive source held at room temperature. For details about the apparatus, sample preparation, ice deposition, and coverage calibration, see Refs. [14–16]. 1 monolayer of ice is defined as 1.15×10^{15} H_2O molecules cm^{-2}.

The two experimental observations underlying the conclusion that photons induce nonthermal crystallization of initially amorphous ice at the graphite-ice interface are as follows: (i) Thermal desorption spectra (TDS) reveal the structure transformation [3,4] through the lower vapor pressure of crystalline ice compared to amorphous ice. (ii) Vibrational spectra by high-resolution electron energy loss spectroscopy (HREELS) reveal a higher coordination of water molecules, i.e., increasing average number of H bonds per H_2O, after irradiation.

Figure 1 shows thermal desorption spectra of H_2O molecules recorded before and after UV irradiation of ice films. The unirradiated ice exhibits a more complex desorption kinetics than the irradiated films. The desorption peak at 138–142 K is attributed to low coordinated water molecules that form the first (2D) layer and/or edge molecules of 3D clusters, while the second peak, with higher desorption energy (lower vapor pressure), corresponds to molecules with higher coordination in 3D clusters. Arrhenius analysis yields an energy difference of 0.13 eV per molecule in the two peaks. (This can with certain assumptions be interpreted as the energy difference between the water-graphite and

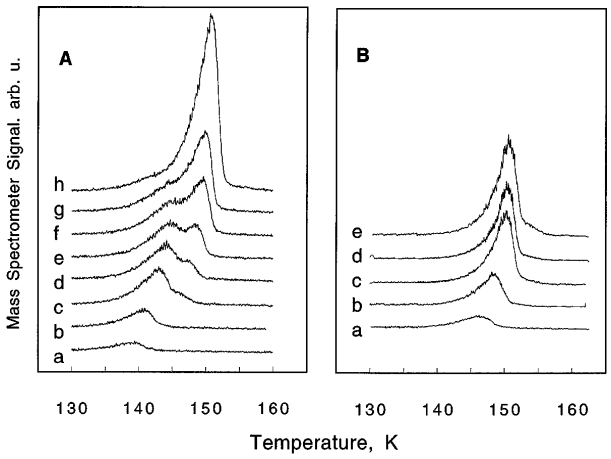

FIG. 1. (A) Thermal desorption spectra of submonolayer H_2O ice depositions on a graphite (0001) surface (MS signal $m/z = 18$), with a linear heating rate of 0.05 $\mathrm{K}\,\mathrm{s}^{-1}$. The coverages are as follows: (*a*) 0.03, (*b*) 0.06, (*c*) 0.14, (*d*) 0.21, (*e*) 0.28, (*f*) 0.37, (*g*) 0.46, and (*h*) 0.83 ML, deposited with rates between 0.004 and 0.012 $\mathrm{ML}\,\mathrm{s}^{-1}$ at 90 K. (B) TDS spectra of UV irradiated deposits, (*a*) 0.05, (*b*) 0.11, (*c*) 0.21, (*d*) 0.28, and (*e*) 0.41 ML. The total photon dose of 8.2×10^{18} photons cm^{-2}, $\lambda = 220–380$ nm [16] is accumulated for 300 s.

the water-water bonds.) These observations support the Stranski-Krastanov growth mode of ice on graphite (0001) as discussed earlier [14,15]. After UV irradiation the TD spectra contain only the high temperature peak; i.e., the amount of (disordered) low coordinated H_2O molecules has diminished. Neither photodesorbing water molecules nor any photodissociation products were detected due to the irradiation as monitored mass spectrometrically and by HREELS, respectively.

HREELS provide additional evidence for the photon-induced structural transformation. Figure 2 shows vibrational spectra of H_2O molecules in the energy region corresponding to the "frustrated" rotations (ν_R) and translations (ν_T), which are known to be sensitive to the H_2O molecule's coordination (number of H bonds) [17,18]. The spectral changes are evidence that the average H_2O coordination increases due to irradiation. The apparent effect of UV irradiation on the HREEL spectra is similar to the effect of thermal annealing [14,15].

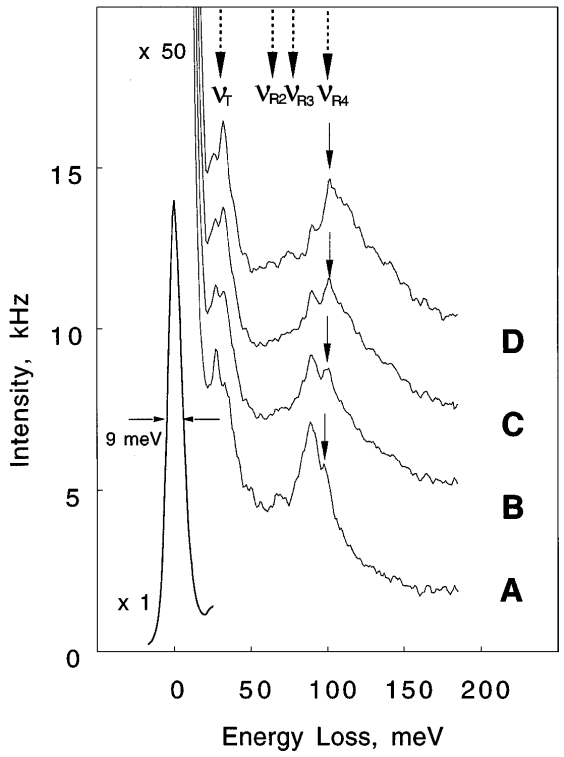

FIG. 2. HREEL spectra of ice on graphite in the region of collective modes. Primary electron energy 6.1 eV; specular scattering at 60°. Spectra *A* and *B* are taken from the same deposition of 0.76 ML. Spectrum *A* is recorded directly after the deposition and spectrum *B* after 100 s UV photon irradiation (total photon dose 2.7×10^{18} photons cm^{-2}). Spectra *C* and *D* are from a separate deposition (0.83 ML), taken after irradiation of the layer for 600 and 1200 s (accumulated photon dose 1.65×10^{19} and 3.3×10^{19} photons cm^{-2}, respectively). The elastic peak belongs to spectrum *D*. The spectra are recorded at 89–90 K. The temperature rise during irradiation was less than 2 K. The dashed lines mark the positions of the corresponding single modes of double, triple, and four coordinated molecules [17,18,28,29].

Preliminary information about the wavelength dependence was obtained by selecting three of the strongest Hg lines at 313, 365, and 440 nm with narrow ($\Delta\lambda \leq 10$ nm) bandpass filters and using an ice coverage of 0.35 ML. Comparing the HREELS spectra taken after the same dose of photons but with different energies, we found that 313 nm irradiation causes almost complete crystallization while no measurable changes were registered after irradiation with 440 and 365 nm photons; i.e., there is a threshold for the observed effect between 365 and 313 nm (3.4–4 eV). The cross section increases rapidly with increasing photon energy.

Similar structure transformations occur also for several monolayers thick films [19]. By measuring the amorphous and crystalline contributions in isothermal TD spectra [3] recorded before and after irradiation, for a large number of ice films of different thickness, we obtained the data in Figs. 3 and 4, summarized as follows: (i) The crystallization effect is linear in photon dose at low doses: (ii) submonolayer coverages can be (almost) completely transformed into the crystalline phase, while multilayers show a saturation for accumulated doses $\geq(2-3) \times 10^{19}$ photons cm^{-2}; and (iii) the thickness dependence of the photon-induced crystallization shows three distinct regimes: (1) The effect of irradiation is strongest below $\sim$0.5 ML (Fig. 4). Here the only limit for complete crystallization into fully coordinated H_2O molecules is probably the limited average number of water molecules that form a cluster; i.e., even if all molecules maximize the coordination number there will still be a significant fraction of edge or surface molecules with low coordination. (2) Photon-induced crystallization is also almost complete for coverage up to 2.5 ML, but with a slower rate. (3) At 3–6.5 ML the effect is still significant, but successively diminishing with increasing thickness.

In our discussion we first note that ice (both amorphous and crystalline) is transparent for visible and near UV photons (see Fig. 5); the optical (electronic) absorption starts above 7 eV, and the first absorption maximum lies at 8.6 eV [20]. Substantial changes in the electronic structure of the H_2O molecules adsorbed on the graphite surface are not likely [14]. Thus, a direct photon interaction with the ice layer is ruled out. Direct optical excitation of H_2O vibrational overtones is also ruled out by the wavelength dependence [21]. Thermal effects due to the cw incident photon flux were carefully measured and found negligible. A thermal mechanism is therefore rejected with strong confidence.

We attribute the photon-induced crystallization to an indirect effect associated with the substrate: Creation of photoexcited charge carriers (electrons or holes) in the graphite surface region is followed by scattering against or into the ice layer. (In the following we discuss only hot electrons [22].) The following facts support this mechanism: (i) Electron scattering against or into ice is a strong dynamic perturbation capable of inducing structural reorientation of water molecules

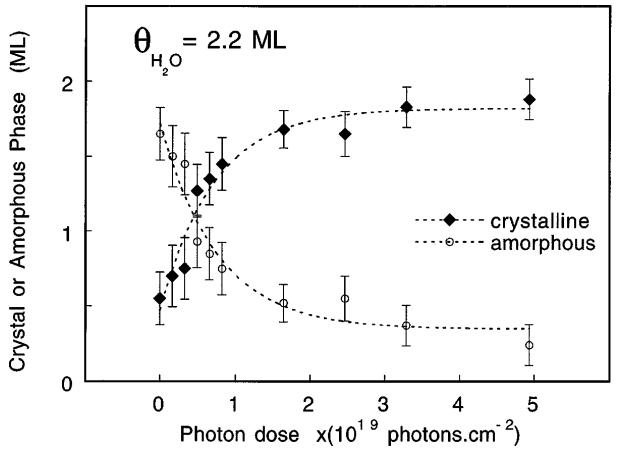

FIG. 3. Crystalline and amorphous ice contributions for 2.2 ML of ice deposited at 90 K on graphite as a function of UV photon dose. The lines are drawn to guide the eye.

[23]. (ii) The successive decline of the crystallization as the ice films become thicker is strong evidence that the perturbation causing crystallization comes from the underlying graphite substrate. (iii) Previous work in our group has demonstrated the importance of such electrons in photodesorption of potassium atoms from graphite [16].

The (photo)electron source under photon irradiation is the graphite substrate. Strong optical absorption of graphite begins around 3 eV and has a first maximum at 4.8 eV (248 nm) due to "vertical" π-π^* interband transitions. There are essentially three mechanisms by which these electrons can induce structural transformations in the ice layer (Fig. 5). They are all based on electron-induced nuclear motions (vibration-rotation-translation) of the H_2O molecules: (i) Inelastic electron scattering against the graphite-ice interface, as in dipole field excitations in a HREELS experiment, but with hot internal electrons below the vacuum level. (ii) Hot electron injection into the conduction band (CB) of ice followed by loss of energy to vibrational-rotational modes. (iii) Electron injection by tunneling to defect related bound states (H_2O^-) in the ice band gap region, i.e., below the CB edge, inducing nuclear motions.

An unambiguous discrimination of these mechanisms is not yet possible, but we favor (iii) with the following arguments: Mechanism (i) is operational but with small efficiency at the present conditions due to the cross section [24]. Mechanism (ii) is less likely on energetic grounds: The CB edge of ice lies close to the vacuum level, about 4–5 eV above the Fermi level (assuming weak band bending), while we observe a threshold at 3.4–4 eV. Since photoexcitations of graphite are strongly dominated by direct, vertical transitions, the majority of the hot carrier energies are $\approx \frac{1}{2}\hbar\omega$, i.e., at most 2 eV above E_F, for photons around the threshold energy. This electron energy is not enough to reach the CB. Only much less probable indirect transitions could produce electrons of sufficient energy. If injection of electrons into the CB were the mechanism, we would expect much thicker films to photocrystallize since at energies above the CB edge there is no tunneling depth restriction.

In mechanism (iii) we take into account that the ice layer in the amorphous state is defect rich and will have diffuse CB and VB edges reminding us of the situation in amorphous semiconductors. Just below the CB edge there will be numerous electron trap states associated with different H_2O (H_2O^-) configurations. A photoexcited graphite electron, with energy $\frac{1}{2}\hbar\omega$ above E_F that reaches the graphite surface can tunnel into these defect states, forming a local and temporary H_2O^- [22,25]. The electron attachment creates a perturbation ($H_2O + e^- \rightarrow H_2O^-$) which induces a nuclear motion (vibrational/rotational excitation) within the local H-bonded network, causing a reorientation to form a new

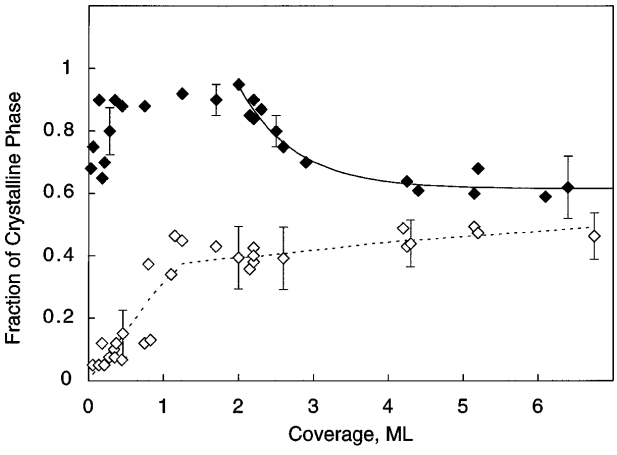

FIG. 4. Fraction of crystalline phase in ice films of different thickness on the graphite surface without (open symbols) and after (solid symbols) UV irradiation; photon dose $(2.28 \pm 0.15) \times 10^{19}$ photons cm^{-2} for each data point. The solid line is an exponential fit; the dashed line is drawn to guide the eye.

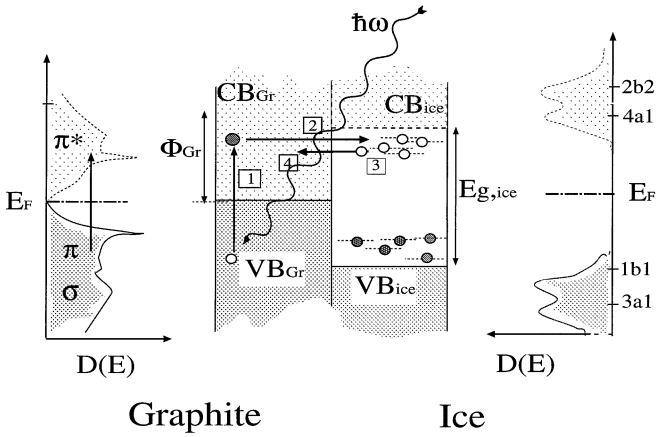

FIG. 5. Schematic energy diagram representation of ice, graphite, and the proposed mechanism for photon-induced crystallization. (1) Photoexcitation of hot electron-hole pairs in graphite bulk; (2) tunneling of the electrons into unoccupied defect states; (3) vibrational/rotational excitation and reorientation induced by electron attachment; (4) return of the electron to the graphite CB. Analogous processes can occur for holes.

H bond with an increase of the local coordination and crystallinity. After some time the electron returns back to the conduction band of graphite. Repeated tunneling—attachment—vibrational excitation—electron return constitutes the overall nonthermal annealing mechanism. For surface molecules on the ice film, the electron attachment can also induce motion as an additional annealing mechanism. However, annealing of defects inside the film is necessary to account for the observed TDS and HREELS spectra.

Our experimental observations are consistent with the interpretation above. The decline of the *relative* amount of photoinduced crystallization as the ice film becomes thicker (Fig. 4) is due to the finite tunneling depth of electrons into the ice layer: As the adlayer thickness increases, photoexcited substrate electrons can eventually not reach the distant (from the graphite-ice interface) H_2O molecules and the crystallization channel closes. The annealing depth can only be estimated, since the original ice film grows via a nucleation-growth procedure and does not completely wet the surface [14]; i.e., the film has laterally varying thickness. Assuming isotropic exponential attenuation we estimate a tunneling depth of $d \approx 3.5$ ML. For comparison Gilton *et al.* [26] observed an attenuation length in water of 4 ML for low energy electrons. Analogous observations were presented by Ukraintsev and Harrison [27].

The ice crystallization mechanism demonstrated here is expected to affect both the gas-solid mass balance and the chemistry of H_2O ice in the outer stratosphere and in space. The details are influenced by the electron structure of the particles on which ice grows and by the UV-irradiation spectrum. For example, much thicker ice films than observed in this work can be crystallized by this mechanism, when the substrate properties and UV light combine to make hot electron injection into the CB of ice possible.

Financial support from the Swedish Research Council for Engineering Sciences (TFR) Contract No. 97-643 is gratefully acknowledged.

*Corresponding author.
Email address: f7xdc@fy.chalmers.se

[1] X. Su *et al.*, Phys. Rev. Lett. **80**, 1533 (1998).
[2] N. Materer, Surf. Sci. **381**, 190 (1997).
[3] P. Löfgren *et al.*, Surf. Sci. **367**, L19 (1996).
[4] R. S. Smith *et al.*, Surf. Sci. **367**, L13 (1996).
[5] W. C. Simpson *et al.*, Surf. Sci. **390**, 86 (1997).
[6] P. V. Hobbs, *Ice Physics* (Clarendon Press, Oxford, 1974).
[7] P. A. Thiel and T. E. Madey, Surf. Sci. Rep. **7**, 211 (1987).
[8] B. J. Gerthner and J. T. Hynes, Science **271**, 1563 (1996).
[9] M. S. Westley *et al.*, Nature (London) **373**, 405 (1995).
[10] N. Materer, J. Phys. Chem. **99**, 6267 (1995).
[11] A. Kouchi, J. Cryst. Growth **99**, 1220 (1990).
[12] N. J. Sack and R. A. Baragiola, Phys. Rev. B **48**, 9973 (1993).
[13] M. C. Festou, H. Rickman, and R. M. West, Astron. Astrophys. Rev. **4**, 363 (1993); **5**, 37 (1993).
[14] D. V. Chakarov, L. Österlund, and B. Kasemo, Langmuir **11**, 1201 (1995).
[15] D. V. Chakarov, L. Österlund, and B. Kasemo, Vacuum **46**, 1109 (1995).
[16] B. Hellsing *et al.*, J. Chem. Phys. **106**, 982 (1997).
[17] D. F. Horning, H. F. Whitte, and F. P. Reding, Spectrochim. Acta **12**, 338 (1958).
[18] K. Nakamoto, *Infrared and Raman Spectra of Inorganic and Coordination Compounds* (John Wiley & Sons, New York, 1986).
[19] The thickness of ice layers that can be probed with HREELS is restricted by charging effects for coverages above several monolayers.
[20] K. Kobayashi, J. Phys. Chem. **87**, 4317 (1983).
[21] G. Herzberg, *Molecular Spectra and Molecular Structure* (D. Van Nostrand, New York, 1964).
[22] Hot holes can operate in a similar way by tunneling into the VB's filled defect states. The relative importance of electrons and holes depends on, e.g., the relative number of n and p type defects in amorphous ice and band bending, factors which are currently not known.
[23] W. C. Simpson *et al.*, J. Chem. Phys. **107**, 8668 (1997).
[24] H. Ibach and D. L. Mills, *Electron Energy Loss Spectroscopy and Surface Vibrations* (Academic Press, New York, 1982).
[25] J. E. Bennett, B. Mile, and A. Thomas, J. Chem. Soc. A **9**, 1393 (1967).
[26] T. L. Gilton, C. P. Denbostel, and L. P. Cowin, J. Chem. Phys. **91**, 1937 (1989).
[27] V. A. Ukraintsev and I. Harrison, Surf. Sci. **276**, 325 (1992).
[28] E. Bertic, L. J. Labbe, and E. J. Whalley, J. Chem. Phys. **49**, 775 (1968).
[29] P. T. T. Wong and E. Whalley, J. Chem. Phys. **64**, 2359 (1976).